The Field Study of Current Estimation for Kuroshio Power-Generating Pilot Facilities

Chang-Wei Lee[#1], Po-Feng Chen[#2], Wan-Ting Chang[#3], Yih Yang[#4], Wen-Chang Yang[#5]

[#]*Taiwan Ocean Research Institute, National Applied Research Laboratories*
Kaohsiung, Taiwan

[1]cwlee@narlabs.org.tw

[2]chenpf@narlabs.org.tw

[3]*wanda@narlabs.org.tw*

[4]yy@narlabs.org.tw

[5]ywc@narlabs.org.tw

ABSTRACT

Ocean current power generation is forward-looking and important in the development of green energy technology. Taiwan Ocean Research Institute deployed an ADCP mooring in a field test site to collect current profile data of upper 500m during August, 2015 to March, 2016. As a whole, the mean current velocities fluctuated highly in the test site due to the reciprocating tidal current in Luzon Strait. Such fluctuations become an unstable situation which may further affect the efficiency of power generation. Therefore, this study suggests to move the power generation site northward to prevent poor efficiency caused by the current instability.

Keywords: Kuroshio, green energy, ADCP mooring, Ocean Current Power Generation

I INTROCUCTION

Global oceans offer an enormous amounts of ocean currents energy. Although it is not widely used at present, technologies are still developed step by step. Ocean current power generation is a potentially important clean energy in the future so that countries of the world are pursuing it. According to th opinion of the European Commission (EC) [1], however, the development of ocean energy technology is still at an early stage when compared with more mature renewable energy technologies such as wind energy or photovoltaics.

Ocean current power generation is forward-looking and important in the development of green energy technology. The ocean energy industry has made significant progress in recent years but is still at a very early stage with some advanced prototypes that are just tested [2]. Research, innovation and enthusiasm can help overcome those barriers.

This paper provides an overview over the current state of research development in the field of ocean energy. In 1992-1993, the Tidal Stream Energy Review identified several specific sites in UK waters with suitable current speed to generate up to 58 TWh/year. It confirmed theoretically that the total marine current power resource were capable to meet 19 % of the UK electricity demand [3]. Verdant Power is conducting performance and environmental monitoring of an array of six horizontal axis turbines in the East River in New York City, USA. If operation and environmental impacts were acceptable, this initial project could lead to an arrangement of around 100 turbines[4]. The New Energy and Industrial Technology Development Organization (NEDO) and IHI Corporation announced on August 25, 2017 that the Kairyu floating system (a 100 kilowatt submerged floating ocean current power generation system) at about 30m to 50m depth can generate up to 30 kilowatts, and maintain its position and depth with an autonomous control system. The trial also produced data on power generation capacity, as well as the stability of the floating structure in an actual ocean area [5], [6].

Looking back at Taiwan, the stable Kuroshio passes through the East of Taiwan and contains the large potential energy for ocean current power generation. Since 2009, WANCHI Steel Industrial Co., Ltd (WANCHI) has been developing the ocean current power generation facility, and had collaborated with Tainan Hydraulics Laboratory (THL) of National ChengKung University, Taiwan Ocean Research Institute (TORI) and National Sun Yar-sen University. The project covers two main aspects: (1) experiment related to power-generating pilot facilities off the coast, and (2) marine environmental impact assessment, including an investigation of how these can be combined to finish team projects successfully.

The experiment site of Kuroshio power-generating pilot facilities is located on the south-eastern sea of Taiwan where is the northern end of Luzon Strait. TORI deployed an ADCP mooring in this site to collect current profile data of upper 500m during August, 2015 to March, 2016 (8 months). The ocean current parameters for the reference information of power-generating pilot facilities can be estimated through the analysis of the long-term current profile data. The main objective of this paper is to analyse and interpret of ocean current data in the epipelagic zone, aiming to increase the overall understanding of marine currents as a renewable energy resource.

II FACILITY SET UP

In order to understand the characteristics of current at the test site, TORI deployed an ADCP mooring to collect long term and time series data of velocity profile in August, 2015. This project aims to measure the current velocity profiles which are referred to the reference parameters of ocean environment background for Power-Generating estimation. Data detection

by the ADCP mooring was proceed during 8 months from August, 2015 to March, 2016.

Considering the bathymetry of field experiment area, the setup of the equipment includes surface buoy with ADCP, attached glass buoys, the length of rope and wire, the calibrated current meter, the gravity anchor, and the acoustic release which should be accurately and carefully assessed. Shown as Figure 1, such pre-preparing work of ADCP mooring was completed by TORI alone.

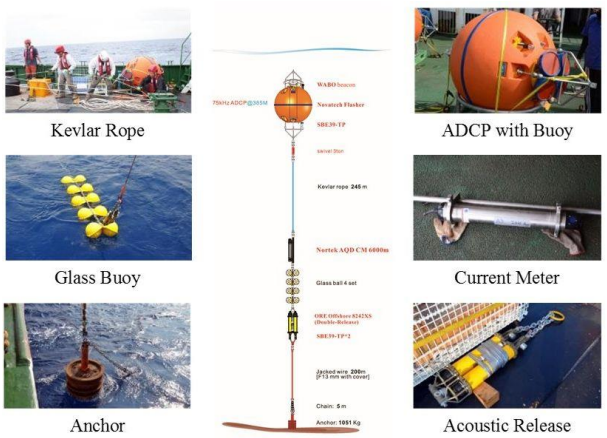

Fig. 1 The design of ADCP mooring

The ADCP with self-recorder was adopted, and the power source of this instrument came from the built-in battery. The data sampling interval optioned by the ping rate depended on the mooring deployment period and battery usage life. Considering site situation and data requirement, the configures of ADCP were setup as Table 1. The range of ADCP mooring detected from 30 m to 525 m in depth for this project. Since the contamination limited by side-lobe effect, the data within 6% of the range near the surface would not be adopted. It indicated that this ADCP could not measure the 30m of upper layer from the surface. The horizontal resolution of velocity profile (cell size) was 4 meter, and the ensemble interval was 10 minutes to collect the better resolution on measuring current velocity and covering the whole upper layer.

Table 1. The operating configures of ADCP setting

Parameter	Value
Ensemble interval	10 (minutes)
Duration	240 (days)
Water pings	16 (pings/Ens)
Cell size	4 (meter)
Number of depth cells	128
Standard deviation	7.25 (cm/s)

The test site selected for the power generating experiment is located at south-east ocean area of Taiwan, shown as Figure 2. The deployment of ADCP mooring was performed by the R/V OR3 from Aug. 2 to 3, 2015. When the R/V OR3 reached the test site, the vessel cruised around this ocean area with oceanographic and topographic surveying at first. The current velocity along the cruise lines and marine topography covering the cruise lines could be detected by shipboard ADCP and single-beam echo sounder.

The project team rode on the R/V OR3 to deploy the ADCP mooring for collecting long-term current velocity profile data to assess the potential of power generating in the test site from Aug. 2 to 3, 2015. The technicians of TORI prepared and inspected the instrument and equipment of mooring such as ADCP, rope, glass buoy, acoustic release, etc., and made programme of mooring deployment during the oceanographic surveying.

The ADCP, rope, glass buoy and current meter were placed into the sea systematically, and the anchor was then released. The distances between the acoustic released and the acoustic transceiver were detected by our technicians to calculate the dropping rate of mooring and the time that the anchor reached sea floor. Figure 2 shows the vessel rode around the mooring and used transceiver to gauge the relative distance for positioning the accurate location of ADCP mooring with triangulation method after anchor located on the seabed.

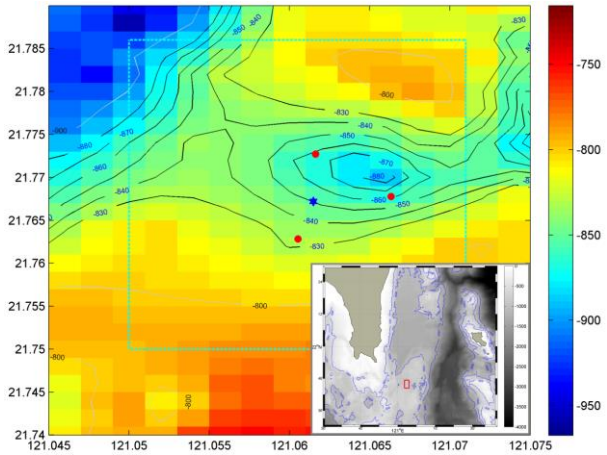

Fig. 2 The bathymetry map of mooring site. The final location of mooring (✶) by triangulation points (●).

For the eight months data collection of ADCP mooring on upper 500 meters, TORI recovered the ADCP mooring by R/V OR3 during March 28 to March 29, 2016. The vessel reached the mooring site at night on March 28, and located the mooring site precisely using triangulation method. After 12 hours current velocity data collection, the vessel then returned to the experimentation site to recovered the ADCP mooring successfully.

III DATA ANALYSIS

Long-term observation and stable sampling rate are two of the advantages of using the ADCP mooring. In order to ensure the data quality and analysing results as the ocean current and tidal motions could affect the measurement of the ADCP, we then executed our Q/A and A/C procedures and discuss the data analysis in this section. We analysed the ADCP data by harmonic and statistic analyse.

3.1 Data Q/A and Q/C

We analysed the ADCP data by following certain Q/A and Q/C procedures. Firstly, time mismatch would to be checked. In fact, time mismatch would happen in some ADCP data. If the time mismatch is not corrected precisely, the time mismatch will be integrated, producing and enlarging errors.

The mooring was tensed by weights and flotations and disturbed by the ocean and tidal currents, causnig mooring sinking (and inclination). The ADCP was assembled by 4 transducers. The included angle between the transducer and the ADCP housing was 20° which limited the inclination angle of the ADCP. This is because when the inclination is over 10°, the data quality of ADCP will seriously downgrade. Figure 3 shows the inclination angle time series of the ADCP in our experiment. The inclination angle was mostly about 1° and below 6°. Consequently, only a very small fraction of data were needed to be flagged, removed and interpolated.

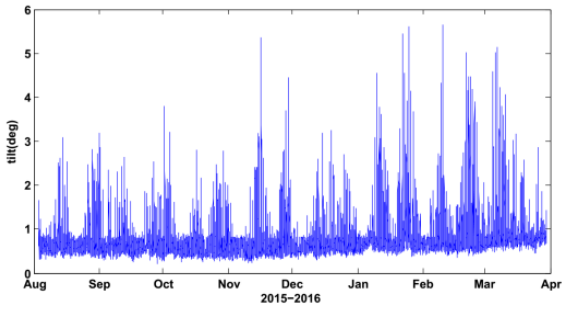

Fig. 3 Tilt of the ADCP on the mooring.

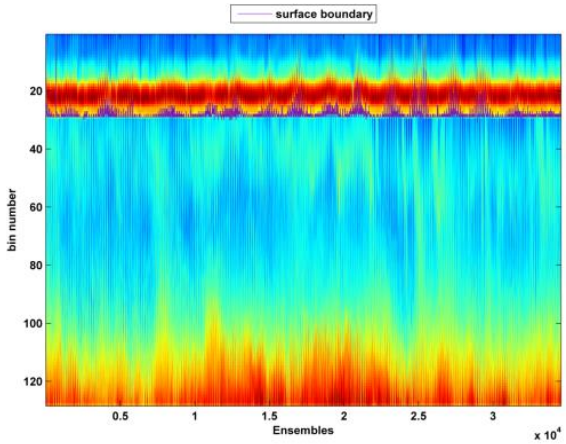

Fig. 4 Echo intensity of ADCP mooring.

In this experiment, the ADCP frequency was 75 kHz which profiling depth was from 40m to 600m in upward looking setting. Considering about the following items: (1) ADCP side-lobe problem, and (2) Mooring sinking and inclination, the ADCP depth was planned to deploy at a depth of 440 m. The percentage of qualified ADCP data is the major threshold of the Q/A and Q/C. Besides that, there was the side-lobe problem near the sea surface boundary. Therefore, the sea surface data with side-lobe problem must be filtered out. Figure 4 shows the ADCP echo intensity, and the purple line shows the boundary between valid and invalid data.

After the procedures mentioned above, the data showed the useful data was 30 m below the sea surface (e.g. Fig. 5). The generator was 20 m below the sea surface. We will then focus on data in 30 m depth.

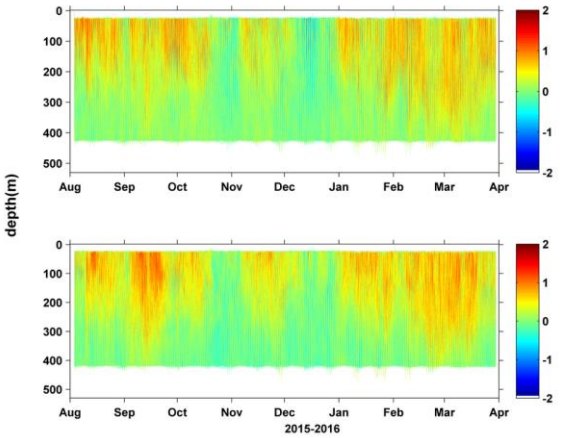

Fig. 5 Raw data of ADCP mooring in U and V component.

ADCP mooring data is composed of periodic tidal current and residual currents. Tidal current is induced by the gravity of Sun or Moon. We separated the tidal current and residual current in the following methods. We focused on the strength and direction stability of tidal current and residual current.

3.2 Tidal current analysis

Fourier transform and spectrum are the common tool in time series analysis which help to identify the static frequency (or period) of time series data. Figure 6 shows the spectrum of U-component in 30 m depth. The significant amplitudes were K1, M2, O1 and S2 in sequence of ascending. The amplitude of M2 and O1 were very close. The complicated bathymetry influenced the tidal current especially near the bottom, which caused the order changing of tidal amplitude.

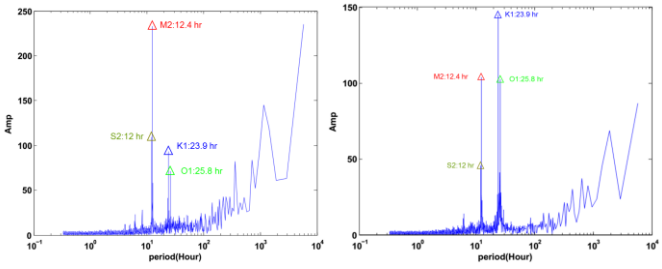

Fig. 6 The spectrum at 30 m and 390 m depth

After spectrum analysis, the harmonic analysis was then applied for cross validation with spectrum analysis. Figure 7 shows the result after the harmonic analysis. The order of amplitudes in the harmonic analysis was M2, S2, K1 and O1, showing a typical tidal constituent. The amplitude of M2 was 0.35 m/s. The amplitude at 390 m depth after harmonic analysis were M2, K1, S2 and O1 (descending sequence). The amplitude of S2 and K1 were similar that also appeared in spectrum analysis. The amplitude of K1 was 0.24 m/s. The result shows that the tidal period at upper layer was semi-diurnal tide, and as

depth ascending it turned to diurnal tide. Figure 8 shows the tidal ellipse of M2, S2, K1 and O1. The ellipse of upper layer was more rounded which means the change of tidal direction was more homogeneous. At 150m depth, the amplitude of M2 was larger than that of K1. As depth ascending the amplitude of M2 was decreasing, oppositely, the amplitude of K1 showed an increasing trend, and the major axis of ellipse turned to NE-SW direction and more elliptic which means that the deeper tidal current was seriously affected by the bathymetry. The major axis of tidal ellipse at depth of closest to the bottom, 690m, was SE-NW direction which was the same as local contour of bathymetry.

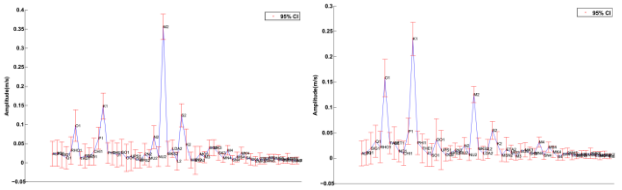

Fig. 7 The results of harmonic analysis at 30 m and 390 m depth

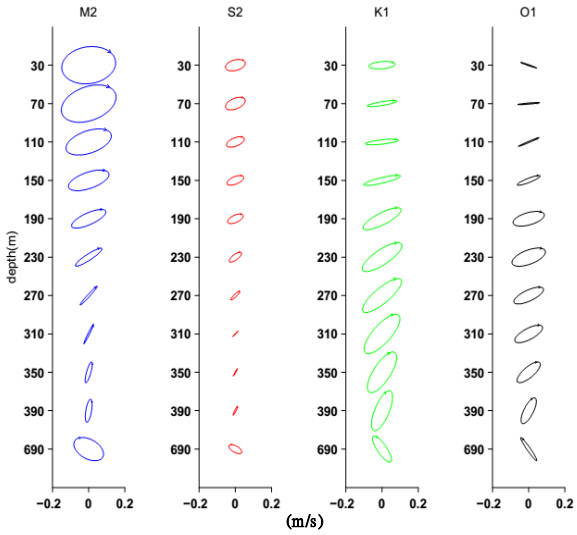

Fig 8 Tidal ellipse of four components

3.3 Residual Current

After spectrum and harmonic analysis, the significant tidal components were identified as semi-diurnal and diurnal tides. The low-pass filter was then applied with 48 hrs cut-off frequency to filter the high frequency noise, tidal and the current. Figure 9 is the time series data after 48-hr low-pass filter. It shows that most of the current directions were south at the depth deeper than 400 m. Therefore, the major current direction was north-east direction at depth of shallower than 300 m. The average current speed was 0.5 m/s at depth of shallower than 100 m/s. The maxima speed is at 50 m depth, and decrease as depth ascending. The speed was almost steady 0.1 m/s at 370 m depth. Some current reversed to south-west or south-east during 2015-10-20 to 2015-12-28. It could be caused by the mid-scale eddy when it arrived at the east of Taiwan. When the strength of eddy was strong enough to compete with Kuroshio, the interaction happened and changed the current speed and direction.

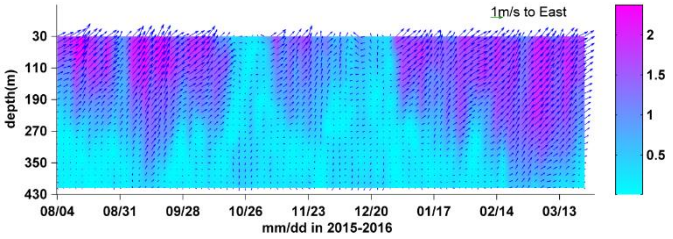

Fig. 9 Current speed and direction after 48hr low-pass filter.

IV RESULTS AND DISCUSSION

The results based on the the spectrum analysis and the hormnoic analysis shows that the main amplitudes was in a descending order of M2, S2, K1 and O1 between the surface and 30 m depth. The order was K1, M2, O1 and S2 at 390 m depth.

The reciprocating motion of the current increased with increasing depth. Once the directions of the long axis was toward the north-south direction, the current ellipse tended to be flattened. Such a result indicated that the influence of bottom terrain on the direction of current increased with increasing depth. The low-frequency flow occasionally weakened or even reversed, but that also rarely happened in the eight-month observation. That is, tidal current constituted the main changes. Figure 10 shows the distributions of velocities and the standard deviations vs. depth. The results show that the changes was mainly contributed by that of the tidal current, especially for the deeper flow. In 30 m, the standard deviation of the westeast flow was 0.34 m/s, which accounted for 77% of the standard deviation of the original flow. The standard deviation of the north-south flow was 0.27 m/s, which accounted for 76% the standard deviation of the original flow. The standard deviations generally decreased with increasing depth, but its proportion in the original velocity increased with decreasing depth. When the water depth reached 410 m, the standard deviation of the eastwest flow was 0.17 m/s, accounting for 90% of the original flow velocity. The standard deviation of the northsouth flow was 0.23 m/s, accounting for 91% of the original flow velocity.

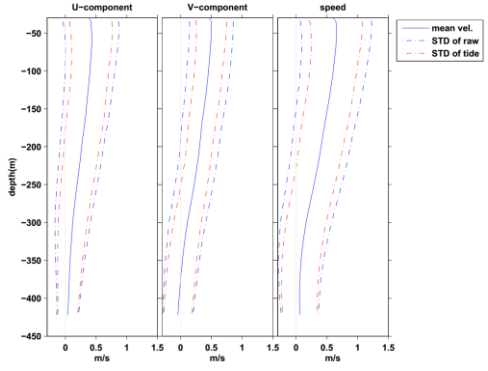

Fig. 10 Distributions of mean and original velocities, as well as their standard deviations

Figure 11 shows the rose images before and after the low-pass filter. After the low-pass filter, we found that there was a stable northeast flow between the surface and 30 m. The situation was similar in 110 m. When the water depth reached to 110 m, the currents before and after the low-pass filter were similar to those at a depth of 30 meters, and the northeast flow was still the dominance. The magnitude of the velocity reduced greatly when the depth reached to 390 m. The directions of the currents was no longer concentrated in the northeast direction as that in the upper layer. The directions were more divergent, but still showed a northeast-southwest pattern. Such results indicated that tide was the main driving force govering the changes in the velocity and direction of the current. After the low-pass filter, the flow in 390 m was not concentrated in the northeast direction as that of the shallower flow. Instead, the directions spread over a wide ranges between 45 and 225 degrees. Our statistical results show that, even at the surface layer, there was no current with a clear direction, such as constantly in the northeast direction.

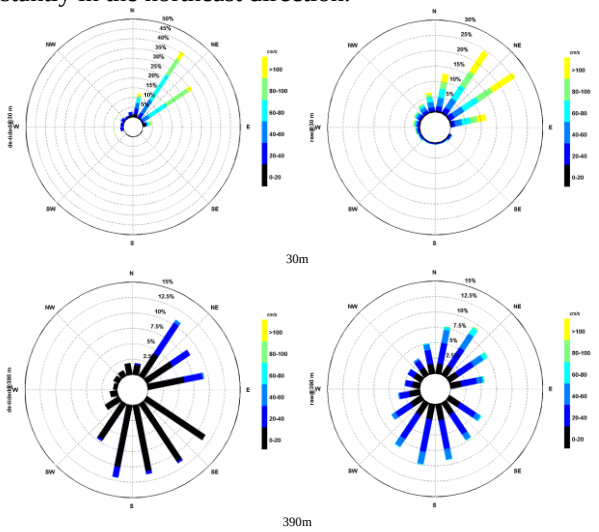

Fig. 11 Rose plot of current and de-tided current in 30 m and 390 m.

The mean currents at various depths were mostly in the northeastern direction, gradually turning eastward with increasing depth, and turning to eastward direction after reaching 380 m. In 43 m (the deepest observation depth for the ADCP), data from the ADCP shows that the current was changed to south-southeast. Data from the flow meter shows that in 695 m, the direction of the flow became west-westsouth. The highest mean velocity was 0.66 m/s in 50 m, and the velocity decreased with increasing depth. The average velocity decreased with depth, and the velocity tended to be stable (within 0.1 m/s) below 370m.

Figure 12. shows the statistical results of the flow in 30 m depth with a time interval of 0.2 m/s. The results show that the flow rate generally agreed the normal distribution, with the interval of 0.5-0.7 m/s being the most (for 50 days). The second was 0.7-0.9 m/s (for 48 days), the number of days reaching 50 days. That is, these two intervals accounted for 42% of the total observation days (240 days). Table 2 lists the details.

Table 2. Number of days for anchored observations in different ranges of velocity.

Velocity (m/s)	<0.1	0.1-0.3	0.3-0.5	0.5-0.7	0.7-0.9
No. of Day	3	22	39	50	48
Velocity (m/s)	0.9-1.1	1.1-1.3	1.3-1.5	1.5-1.7	>1.7
No. of Day	37	25	11	4	1

The current velocity of the ADCP data that measured in 240 days had proved the normal distribution shown in Fig. 10. The days of current speed between 0.5 to 0.9 m/s was 98 days that occupied the 42% of total observation days by the ADCP mooring, shown as Figure 12.

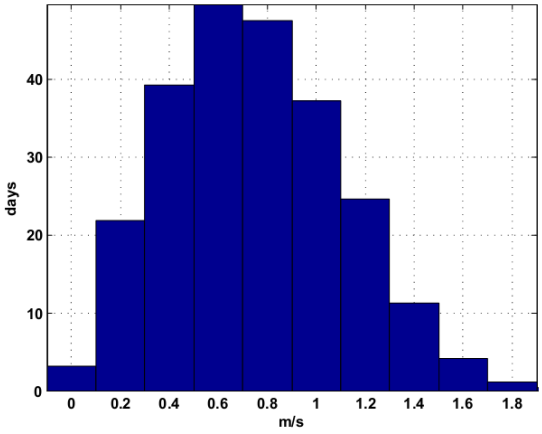

Fig. 12 The dates statistics of current velocity by mooring observation.

V CONCLUSION

Understanding the characteristic of current field in the sea area is critical before setting up the ocean current power generator. TORI deployed an ADCP mooring in the site where was on the south-eastern sea of Taiwan to collect current profile data of upper 500m during 8 months from August, 2015 to March, 2016. The current profile data were analyzed.

In order to obtain the efficient current component, a low-pass filter was applied to remove high frequency motion such as the tidal component, and then extracted the low-frequency current which would efficiently work for power generation. The results of the estimated velocity profiles above 300 m showed that the direction approached northeast and the average current speed was 0.5 m/s. Meanwhile, the maximum current speed was 0.66 m/s at 50 m depth and decreased with depth until 370 m depth the current tended stably within 0.1 m/s.

The time series data of current velocity profile showed the current at 30 m depth was northeast flow and the maximum speed reached 1.2 m/s where stability coefficient was about 0.85 (if stability coefficient was 1, means that the current was very stable without any variation). Although the mean current in this sea area was northeast during the ADCP observation, the current speed decreased significantly in several days even the

current direction changed to southward. The cause of those incident was primarily related to the significant mesoscale eddies in the eastern sea of Taiwan [8], but the exact factor needs more data to discuss in the future study.

As a whole, the mean current velocities fluctuated highly in the test site due to the reciprocating tidal current in Luzon Strait sea area. Such a velocity fluctuation become an unstable situation that may further affect the efficiency of power generation. Finally, the suggestion of this study is to move the site of power generation northward to prevent poor efficiency caused by the current instability.

ACKNOWLEDGMENT

This project of current estimation research was supported by MOST (Ministry of Science and Technology, R.O.C) and WANCHI Steel Industrial Co., Ltd of foundation. Expressed the deepest appreciation to all of the colleagues who provided insight and expertise that greatly assisted the research.

REFERENCES

[1] D. Magagna and A. Uihlein (2015). *2014 JRC Ocean Energy Status Report*. Publications Office of the European Union, EUR 26983 EN.

[2] A. Uihlein and D. Magagna (2016). Wave and tidal current energy – A review of the current state of research beyond technology, *Renewable & Sustainable Energy Reviews*, vol. 58, pp. 1070-1081.

[3] Ponta, F. L., & Jacovkis, P. M. (2008). Marine-current power generation by diffuser-augmented floating hydro-turbines. Renewable energy, 33(4), 665-673.

[4] Office of Energy Efficiency and Renewable Energy. (2009). *Report to Congress on the Potential Environmental Effects of Marine and Hydrokinetic Energy Technologies*, U.S. Department of Energy.

[5] NEDO and IHI Conduct World's First Trials of 100 kW Ocean Current Power Generation System. (2017, Nov. 29). *Japan For Sustainability*. Retrieved from https://www.japanfs.org/

[6] P. Charlier (2017, Aug. 22). Taiwan Scientists Challenge Japan on Kuroshio Current Energy Claims: We Were First. *Taiwan English News*. Retrieved from http://taiwanenglishnews.com/

[7] Gordon, R. L., & Instruments, R. D. (1996). Principles of operation a practical primer. RD Instruments, San Diego.

[8] Yang, Y., Liu, C. T., Hu, J. H., & Koga, M. (1999). Taiwan Current (Kuroshio) and impinging eddies. Journal of Oceanography, 55(5), 609-617.